







An Experimental Alternative of Microwave Signal Generation through an Optical Heterodyning Technique Using a Multimode Laser Diode and a Tunable DFB Laser

Blaise Tshibangu-Mbuebue , Min Won Lee , Alejandro García-Juárez , Edgard Y. Tshishimbi-Kanyinda , Roberto Rojas-Laguna , and Ignacio Enrique Zaldívar-Huerta 

Abstract—Experimentally, an alternative technique to one of the classical optical heterodyning methods for generating microwave (MW) signals is demonstrated. The novelty of this approach lies in the utilization of a Multimode Laser Diode (MLD) in conjunction with a Fiber Bragg Grating (FBG) and a tunable Distributed Feedback (DFB) laser, rather than employing two DFB lasers. The FBG acts as an optical filter, enabling the selection of only one mode of the MLD. This selected mode serves as a reference in the optical beating process alongside the signal from the tunable DFB laser. Tuning is achieved by varying the wavelength of the DFB laser to modify the wavelength separation ($\Delta\lambda$) between the two optical modes. Experimental results are corroborated theoretically and through simulation. Performance evaluation of the system is conducted by measuring the signal-to-noise ratio (SNR) and the Phase Noise (PN) parameters.

Link to graphical and video abstracts, and to code: <https://latam.ieceer9.org/index.php/transactions/article/view/8596>

Index Terms—Fiber Bragg Grating, Microwave Signal Generation, Optical Beating, Optical Heterodyning, Tunable Distributed Feedback Laser.

I. INTRODUCTION

In communication systems, the generation of microwave (MW) signal generation is of great interest due to its role as an electrical carrier for information transport. Currently, photonic technology is focused on obtaining electrical signals in the microwave range to enhance the quality of high-speed communication systems such as radar, 5G network, Internet of Things, and artificial intelligence, among others [1], [2]. The continuous increase in demand for data traffic has made this a significant challenge for technology services.

This work was supported by the project SEP-CONAHCYT-ANUIES (299017), and the ECOS-Nord program (M19P03).

B. Tshibangu-Mbuebue and I. E. Zaldívar-Huerta are with the Instituto Nacional de Astrofísica, Óptica y Electrónica, Tonantzintla, Puebla, México (e-mails: bmbuebue@inaoep.mx and zaldivar@inaoep.mx).

M. W. Lee is with the Université Sorbonne Paris Nord, Villetaneuse, France (e-mail: min.lee@univ-paris13.fr).

A. García-Juárez is with the Universidad de Sonora, Hermosillo, México (e-mail: alejandro.garcia@unison.mx).

E. Y. Tshishimbi-Kanyinda is with the Institut Supérieur de Techniques Appliquées, Kinshasa, RD Congo (e-mail: tedtshishimbi@gmail.com).

R. Rojas-Laguna is with the Universidad de Guanajuato, Salamanca, México (e-mail: rlaguna@ugto.mx).

A recent survey reports that the global mobile network traffic including Fixed Wireless Access (FWA) reached 118 Exabyte (EB)/month at the end of the year 2022 and is projected to reach 472 EB/month at the end of 2028 [3]. Fig. 1 illustrates a decade projection statistic of the global network traffic since 2018.

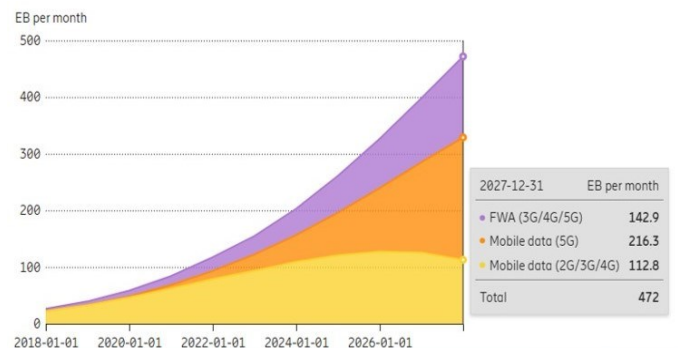


Fig. 1. Global mobile network data traffic (image source: LM Ericsson [3]).

The performance of services demanded by end-users in communication systems is often limited by the capacities of traditional technology resources. Hence the generation of microwave (MW) signals is of vital importance. In this regard, it is well known that microwave signal generation can be realized using oscillators based on electronic devices such as Gunn diodes or transistors [4], [5]. However, sometimes these methods fail to produce satisfactory results. Thus, several approaches for generating MW signals by optical techniques have emerged. Currently, there are several optical techniques to generate microwave signals, such as 1) Heterodyning two optical signals in a nonlinear optical crystal. 2) Heterodyning of two optical signals in a fast photodetector. 3) Opto-electronic oscillator, and 4) Mode-locked lasers. Each technique has its particular characteristics, the simplest being the heterodyning of two optical signals in a fast photodetector [6]. The interested reader can find a full comparison of these techniques in this last reference. In particular, in the optical heterodyning technique, two optical waves with different wavelengths are beating at a photodetector to produce an electric beat frequency corresponding to the frequency spacing of the two optical waves [7] [8] [9]. Even more, in [8] it is shown the capability of tuning for the generated MW signals by using a fixed and a tunable DFB. Difference of this work, this article shows a novel

technique where the use of a Multimode Laser Diode (MLD) in conjunction with a Fiber Bragg Grating (FBG) allows the replacement of a DFB laser. To the best of our knowledge, this represents the original application of this technique. This methodology enables MW signal generation within the frequency range of 1 GHz to 20 GHz. To evaluate the performance of this approach, the signal-to-noise ratio (SNR) and Phase Noise (PN) parameters are computed. Experimental results are contrasted with theoretical and simulated outcomes, with simulations conducted using VPIphotonics software [10]. The subsequent sections delineate the fundamental principles of optical heterodyning, followed by the presentation of our proposed MW signal generation method and its results. Finally, we summarize the main points of this study in the conclusion section.

II. FUNDAMENTAL PRINCIPLE

A. Optical Heterodyning

The fundamental principle of optical heterodyning, often termed ‘‘optical beating’’, involves the synthesis of MW signals by merging two light waves. This combination produces an optical signal containing spectral components corresponding to the frequency separation between the two waves [9].

In Figure 2, the process of optical heterodyning is visually depicted. Two independent lasers emit light waves characterized by wavelengths λ_1 and λ_2 (or frequencies f_1 and f_2), respectively. These waves undergo combination through an optical combiner (OC) before being injected into a photodiode (PD). The result is the generation of an MW signal with a frequency value f_{MW} , directly proportional to the difference in frequency between the two combined light waves.

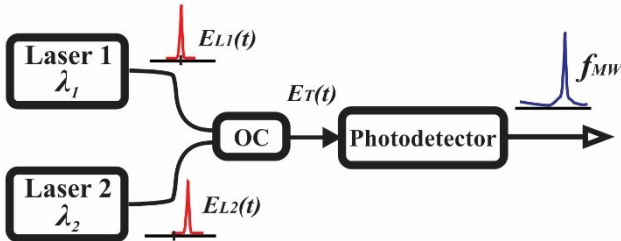


Fig. 2. Basic diagram of optical heterodyning.

Assuming ideal lasers delivering monochromatic signals (zero-linewidth), their optical fields are expressed as [7]

$$E_{L1}(t) = E_{01} \exp[j(2\pi f_1 t + \phi_1)], \quad (1)$$

$$E_{L2}(t) = E_{02} \exp[j(2\pi f_2 t + \phi_2)]. \quad (2)$$

At the output of the OC, the combined total field is

$$E_{LT}(t) = E_{01} \exp[j(\omega_1 t + \phi_1)] + E_{02} \exp[j(\omega_2 t + \phi_2)]. \quad (3)$$

where $\omega = 2\pi f$, E_{01} and E_{02} are the amplitudes, ϕ_1 and ϕ_2 are the random phases of the two lasers, respectively.

The combined optical signal applied to the PD generates a photocurrent I_{PMW} that is directly proportional to the square of the applied field (square-law device) determined by

$$\begin{aligned} I_{PMW} &= |E_{LT}(t)|^2 \\ &= E_{LT}(t) E_{LT}^*(t) \\ &= E_{01}^2 + E_{02}^2 + 2E_{01}E_{02} \cos(\omega_1 - \omega_2)t + (\phi_1 - \phi_2), \quad (4) \end{aligned}$$

$$\text{with } \cos \theta = [\exp(j\theta) + \exp(-j\theta)]/2.$$

Assuming that the squared terms correspond to the PD direct current and an identical polarization for laser light waves, the photocurrent can be expressed as

$$I_{PMW} = RS|E_{LT}(t)|^2 = 2RSE_{01}E_{02} \cos(2\pi\Delta\nu)t + \Phi. \quad (5)$$

R and S are the responsivity and sensitive area (A/W) of the PD; $\Delta\nu = \omega_1 - \omega_2$ and $\Phi = \phi_1 - \phi_2$ are the beat frequency and phase of the generated MW signal.

The generated MW frequency f_{MW} is equal to the beat frequency $\Delta\nu$ that corresponds to the difference of optical frequencies of the two lasers, also known as the Intermediate Frequency (IF) expressed as

$$\Delta\nu = f_{MW} = |f_1 - f_2| = \frac{\Delta\lambda \cdot c}{\lambda_1 \lambda_2} \Leftrightarrow \frac{|\lambda_1 - \lambda_2|c}{\lambda_1 \lambda_2}. \quad (6)$$

$\Delta\lambda$ is the absolute value of the independent laser wavelength difference, and c is the speed of the light in the vacuum; where $f = c/\lambda$.

For a non-ideal laser, delivering a non-strictly monochromatic signal, there is a presence of phase noise. The optical field is not a line spectrum and can be expressed as

$$\begin{aligned} E_{Ln1}(t) &= E_{0n1} \cos[(2\pi f_{n1}t) + \phi_{n1}(t)] \\ &= E_{0n1} \{ \cos(2\pi f_{n1}t) \cos[\phi_{n1}(t)] - \\ &\quad \sin(2\pi f_{n1}t) \sin[\phi_{n1}(t)] \}. \quad (7) \end{aligned}$$

Considering the phase noise $\phi_n(t)$ negligible for both lasers, we have:

$$E_{Ln1}(t) \cong E_{0n1} \{ \cos(2\pi f_{n1}t) - \sin(2\pi f_{n1}t) \sin[\phi_{n1}(t)] \}, \quad (8)$$

$$E_{Ln2}(t) \cong E_{0n2} \{ \cos(2\pi f_{n2}t) - \sin(2\pi f_{n2}t) \sin[\phi_{n2}(t)] \}. \quad (9)$$

Finally, the phase noises are still associated with the laser frequencies f_n , generating lateral bands around it and exhibiting a spectrum with a finite non-zero linewidth. Assuming $E_{0n1} = E_{0n2} = I$ and considering only difference frequency terms, the combined signal crossing the PD results in a photocurrent given by

$$\begin{aligned} I_{PMWn} &= RS|E_{LTn}(t)|^2 \\ &= RS \{ E_{0n1} \{ \cos(2\pi f_{n1}t) - \sin(2\pi f_{n1}t) \sin[\phi_{n1}(t)] \} \\ &\quad + E_{0n2} \{ \cos(2\pi f_{n2}t) \\ &\quad - \sin(2\pi f_{n2}t) \sin[\phi_{n2}(t)] \} \}^2 \\ &= RS [\cos(2\pi\Delta\nu)t - \phi_{n1}(t)\phi_{n2}(t) \cos(2\pi\Delta\nu)t \\ &\quad - \phi_{n1}(t) \sin(2\pi\Delta\nu)t \\ &\quad + \phi_{n2}(t) \sin(2\pi\Delta\nu)t] \\ &= RS \{ \cos(2\pi\Delta\nu)t [1 - \phi_{n1}(t)\phi_{n2}(t)] - \\ &\quad \sin(2\pi\Delta\nu)t [\phi_{n1}(t) - \phi_{n2}(t)] \} \quad (10) \end{aligned}$$

The sum and product of the frequency components are not contained in the bandwidth range of the PD.

B. Optical Filter: Fiber Bragg Grating

The operation of an FBG is based on the principle of “Fresnel reflection” that appears when a light wave is subjected to a change in the refractive index during its propagation in a waveguide [11]. Fiber gratings are longitudinal periodic or aperiodic disturbances on the index profile produced on a short part of a fiber core, allowing perturbations of its refractive index. Each gap of the grating back reflects a particular mode field that interferes constructively and forms a considerable reflected light known as Bragg reflection. The propagating light-wave field E_p is characterized by a transversal field profile E and a propagating constant k expressed as

$$E_p = E(r, \varphi)e^{-j(\omega t - kz)}, \quad (11)$$

$$k = \frac{2\pi n_{eff}}{\lambda}. \quad (12)$$

here, r is the radial direction, φ is the azimuthal direction, ω is the radial frequency, and z is measured longitudinally along the fiber. n_{eff} is the effective refractive index of the grating in the fiber core and λ is the vacuum wavelength.

There are different construction methods and structures of FBGs. For uniform structures, the Bragg wavelength (λ_{BG}) which is a reflected mode, is given by

$$\lambda_{BG} = 2n_{eff}\Lambda_{BG}, \quad (13)$$

with Λ_{BG} the grating modulation period.

Indeed, the Fiber Bragg Grating (FBG) ideally reflects a specific wavelength of the incident spectrum and transmits all others. Figures 3a and 3b illustrate the principle of operation of this device. Connecting a three-port optical circulator (Cr) to the FBG enables the retrieval of transmitted and reflected light waves from an incident light beam.

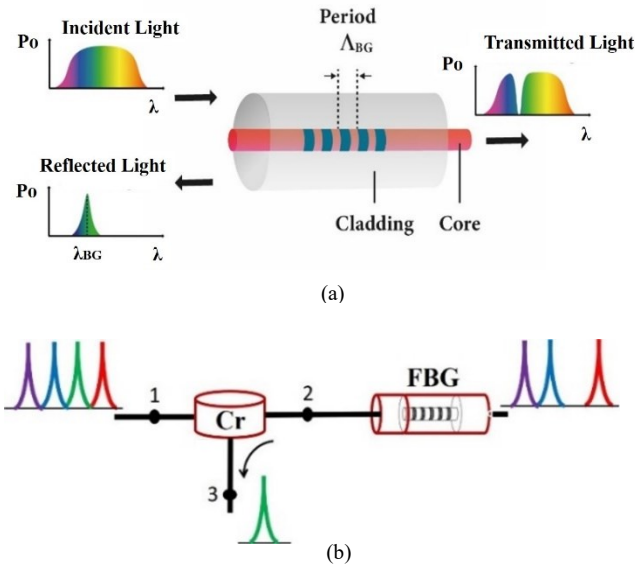


Fig. 3. Operation principle of the FBG: (a) structure, and (b) Illustrative representation of the functioning of an FBG.

The incident light feeding the circulator is transferred from port 1 to port 2 and then injected into the FBG. One part of the light

is transmitted and the other part is reflected returning to port 2 and forwarded to port 3. Fig. 4a shows the transmitted optical spectrum corresponding to a commercial MLD (Anritsu MU951001A) injected into an FBG characterized by its Bragg wavelength $\lambda_{BG} = 1550.32$ nm. Fig. 4b corresponds to the reflected optical spectrum, remarking the presence of only a mode. In both cases, the optical spectrums are registered by an Optical Spectrum Analyzer (OSA).

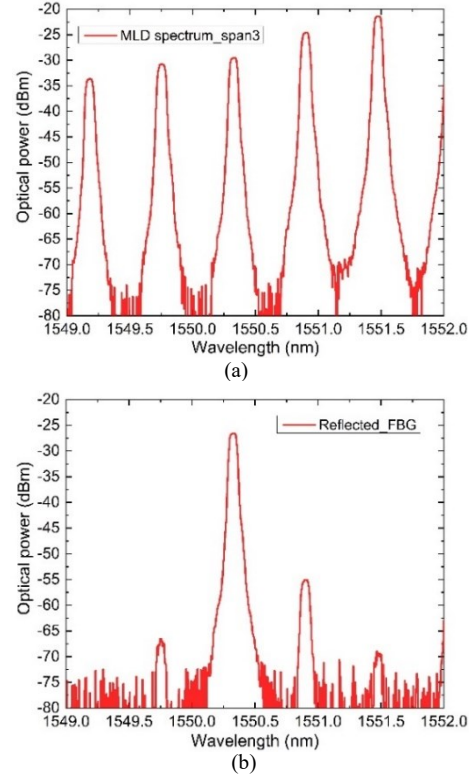


Fig. 4. Optical spectrum of (a) the incident light from the MLD; (b) the FBG reflected light ($\lambda_{BG} = 1550.32$ nm).

III. PROPOSAL OF MW SIGNAL GENERATION AND RESULTS

As established earlier, this work aims to generate MW signals using optical heterodyning. The proposed method utilizes an MLD and a tunable DFB laser, deviating from the conventional use of two DFB lasers. Additionally, we demonstrate the tunability of the generated MW signals. Experimental validation of this proposal is supported by theoretical and simulated results. The following subsections provide a detailed description of the simulations, followed by an explanation of the experimental setup. Finally, a summary of the results is presented.

A. Simulated Setup

The simulation is conducted using VPIphotonics software, a powerful platform dedicated to designing, testing, and optimizing various types of electro-optical systems. Figure 5 illustrates the simulated setup, where the MLD source comprises a nine-laser array coupled to a 9x1 power combiner (enclosed in the blue box). A wavelength of 1550.32 nm from one of the continuous wave lasers aligns with the Bragg wavelength of the FBG. As a result, it is reflected and serves as the reference value in the optical beating process. Simulation

parameters are selected based on the characteristics of the devices available in our laboratory.

Depending on the type of signal to be displayed, optical or electrical, virtual signal analyzers play the role of Optical Signal Analyzer (OSA) or Electrical Spectrum Analyzer (ESA), respectively.

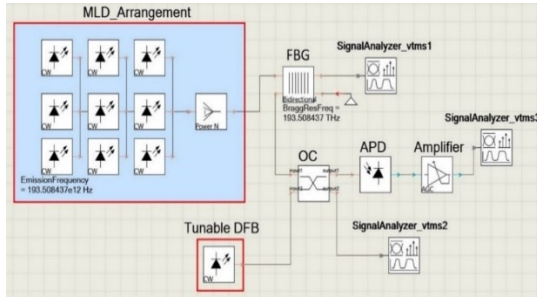


Fig. 5. Layout of the proposal scheme for MW signals generation.

Fig. 6a and 6c show two combined light signals separated by the distance $\Delta\lambda$ of 0.01 nm and 0.16 nm, respectively. Whereas Fig. 6b and 6d illustrate their corresponding MW signals generated, 1.25 GHz and 20 GHz, respectively.

B. Experimental Setup

Fig. 7 shows the experimental setup used to carry out the generation and tuning of a MW signal. The wavelengths (1550 nm) of the optical sources used in this experiment correspond to the wavelengths used in the current optical communication systems. In particular, the use of this wavelength is the region where optical fibers have small transmission loss. On the other side, a possible affectation to this proposed system is a feasible variation of the central wavelength of the optical sources, to prevent this, the optical sources are driven by current and temperature controllers to guarantee a stable emission. The light issued by the MLD passes from ports 1 to 2 of the Cr and is injected into the FBG. This optical signal is displayed on the OSA. The reflected light (λ_1) in the FBG travels from ports 2 to 3 of the Cr and is coupled to one of the inputs of the OC which also receives the light coming from the tunable DFB (λ_2). Thus, the output of the OC contains the two optical signals separated by the distance $\Delta\lambda$. This optical signal is injected into the PD delivering the corresponding MW signal, amplified, and visualized on the ESA.

Fig. 8a and 8c show two combined light signals separated by the distance $\Delta\lambda$ of 0.01 nm and 0.16 nm, respectively. Whereas Fig. 8b and 8d depict their corresponding MW signals generated, 1.46 GHz and 19.31GHz, respectively.

The measured SNR for these MW signals, 1.46 GHz and 19.31 GHz is 34.65 dB and 29.64 dB, respectively. In particular, for the MW signal located at 1.46 GHz, its phase noise measure at 100 MHz-offset frequency is analytically determined by using the analyzer method, obtaining -88.16 dBc/Hz.

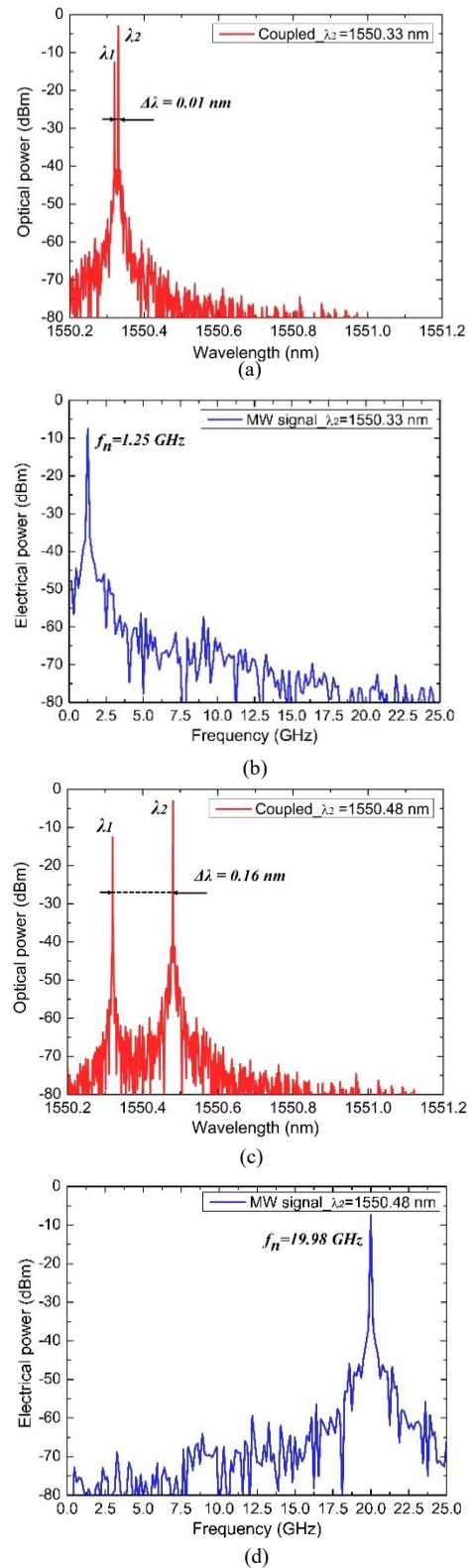


Fig. 6. Simulated combined optical signals and the generated MW signal. (a, b) at $\lambda_2 = 1550.33$ nm, $\Delta\nu = 1.25$ GHz; and (c, d) at $\lambda_2 = 1550.48$ nm, $\Delta\nu = 20$ GHz.

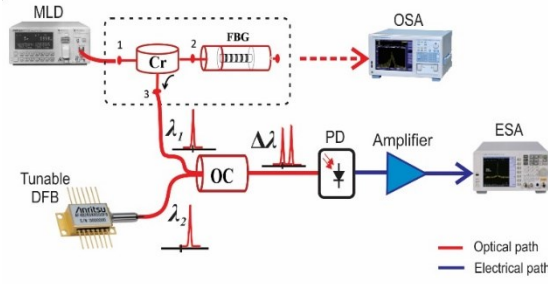


Fig. 7. Experimental scheme for MW signals generation.

C. Tunability of the System

Tuning of the MW signal is demonstrated by varying automatically λ_2 from 1550.33 nm to 1550.48 nm, obtaining an $\Delta\lambda = 0.15$ nm range of 0.15 nm. Fig. 9a and 9b show the obtained spectrum maps for the laser variations and the generated MW signals, respectively.

Reliant on the $\Delta\lambda$ variations, tuning of the generated MW signal follows a linear behavior. Seeing as reference $\lambda_1 = 1550.32$ nm, the adjustment of λ_2 provokes the variation of $\Delta\lambda$ and therefore the tuning of the generated MW signal. Table I tabulates the theoretical (f_{th}) (by the use of (6)), simulated (f_n), and experimental (f_m) results corresponding to the MW signals obtained.

TABLE I
SUMMARY OF THEORETICAL, SIMULATED, AND EXPERIMENTAL RESULTS
CORRESPONDING TO THE MICROWAVE SIGNALS OBTAINED

λ_1 (nm)	λ_2 (nm)	$\Delta\lambda$ (nm)	f_{th} (GHz)	f_n (GHz)	f_m (GHz)	%error
1550.32	1550.33	0.01	1.24	1.25	1.46	17.74
	1550.34	0.02	2.49	2.50	2.45	1.60
	1550.35	0.03	3.74	3.75	3.32	11.22
	1550.36	0.04	4.98	5.0	4.35	12.65
	1550.37	0.05	6.23	6.25	6.29	0.96
	1550.38	0.06	7.48	7.5	7.17	4.14
	1550.39	0.07	8.73	8.75	8.20	6.07
	1550.40	0.08	9.97	10.0	9.19	7.82
	1550.41	0.09	11.22	11.25	11.20	0.17
	1550.42	0.1	12.47	12.5	12.18	2.32
	1550.43	0.11	13.72	13.75	13.26	3.35
	1550.44	0.12	14.96	15.0	14.23	4.87
	1550.45	0.13	16.21	16.25	16.17	0.26
	1550.46	0.14	17.46	17.5	17.21	1.43
	1550.47	0.15	18.7	18.75	18.27	2.29
	1550.48	0.16	19.95	20.0	19.31	3.20

From the tabulated values, it is observable that theoretical (f_{th}) and simulated (f_n) results are very close between them. Not thus for the experimental results (f_m), therefore, the percent error between the theoretical and experimental results is computed as

$$\%error, e = \frac{|f_n - f_m|}{f_n} \times 100, \quad (14)$$

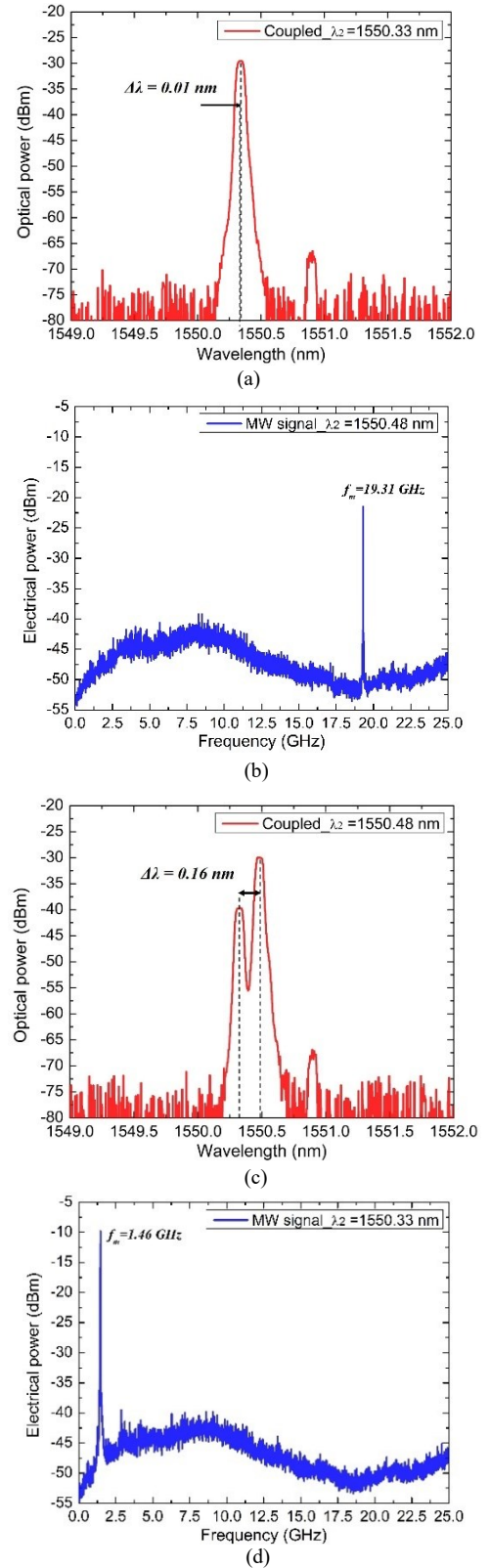


Fig. 8. Experimental combined optical signals and the generated MW signal: (a, b) at $\lambda_2 = 1550.33$ nm, $\Delta\nu = 1.46$ GHz; and (c, d) at $\lambda_2 = 1550.48$ nm, $\Delta\nu = 19.31$ GHz.

On average a 5 % difference between the theoretical and experimental results is obtained. Given that the maximum and minimum values of error are 17.74 and 0.178, respectively, the value of 5 % can be considered acceptable for the experimental results.

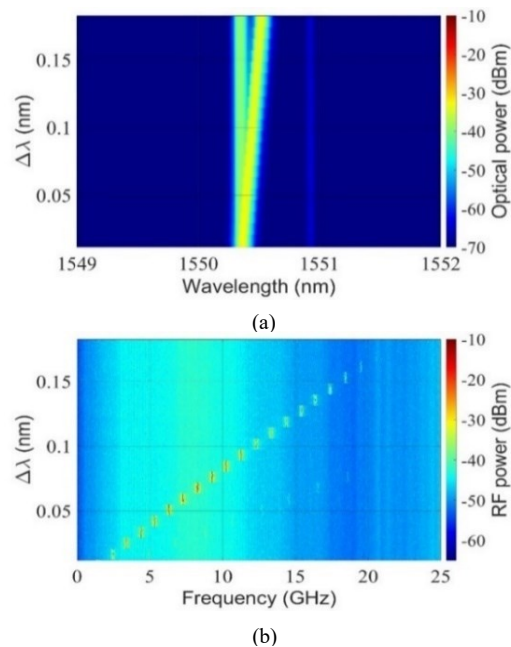


Fig. 9. Spectrum map of (a) $\Delta\lambda$ variations, and (b) generated Microwave signal.

IV. CONCLUSION

The successful demonstration of generating MW signals using an MLD and a tunable DFB laser instead of the two DFB lasers commonly reported in literature signifies a significant advancement. To our knowledge, this technique has not been proposed before. Furthermore, we have demonstrated the tunability of the generated MW signals, aided by the use of an FBG. This approach enabled the generation of MW signals across the frequency range from 1 GHz to 20 GHz. The performance evaluation of this proposal utilized SNR and PN parameters, yielding an average SNR of 30 dB and phase noise of -88.21 dBc/Hz@100 MHz. Experimental results were compared with theoretical and simulated outcomes, showing good agreement with those reported in the literature [7] [8] [9].

A technical limitation of using an FBG as an optical filter to select only one optical mode from the several modes comprising an MLD is that the selection depends on the Bragg wavelength (λ_{BG}) characterizing this optical device. This implies that a specific Bragg wavelength must be selected whenever a particular optical mode is desired. Another restriction is that the available electrical bandwidth of the PD used imposes the maximum limit to obtain the MW signals. These technical limitations can be solved in future research using an FBG with different Bragg wavelengths to obtain a particular tuning value of the MW signals, as well as, a PD with a large electrical bandwidth to extend the frequency range of work. Our proposal demonstrated successfully an alternative to the classical heterodyning technique. Instead of using two DFB

sources, an MLD in conjunction with a DFB was used. Even more, the good agreement between simulation and experimental results guarantees good robustness to this proposal. In addition, potential applications of microwave signals generated by electro-optical techniques lie in the fields of instrumentation, engineering, and medicine, among others [12] [13] [14].

ACKNOWLEDGMENTS

Blaise Tshibangu-Mbuebue expresses deep gratitude to the Mexican Consejo Nacional de Humanidades, Ciencias y Tecnología (CONAHCyT) for the PhD scholarship number 846218.

REFERENCES

- [1] De. Sampurna, A.A. Bazil Raj, "A survey on photonics technologies for radar applications," *J Opt* 52, 90–119 (2023). <https://doi.org/10.1007/s12596-022-00897-x>
- [2] Y. Zhou, L. Wang, Y. Liu, Y. Yu, X. Zhang, "Microwave Photonic Filters and Applications," *Photonics* 2023, 10, 1110. <https://doi.org/10.3390/photonics10101110>
- [3] Telefonaktiebolaget LM Ericsson 1994-2023, "Mobile data traffic outlook," [Online]. Available: <https://www.ericsson.com/en/reports-and-papers/mobility-report/dataforecasts/mobile-traffic-forecast>
- [4] I. Storozhenko, "Advanced Gunn Diode on Based Graded GaPAs - GaInAs as High Power Source of Millimeter Wave," 2021 IEEE Microwave Theory and Techniques in Wireless Communications (MTTW), Riga, Latvia, 2021, pp. 111-116, doi: 10.1109/MTTW53539.2021.9607065
- [5] R. León, C. Rosero, A. F. Tinoco-S, G. Guarderas and F. Lara, "Low Cost mmWaves Electromagnetic Spectrum Monitoring System for Education and Research Purpose," 2022 IEEE 7th Forum on Research and Technologies for Society and Industry Innovation (RTSI), Paris, France, 2022, pp. 38-42, doi: 10.1109/RTSI55261.2022.9905192.
- [6] A. Madjar and T. Berceli, "Microwave Generation by Optical Techniques - A Review," 2006 European Microwave Conference, Manchester, UK, 2006, pp. 1099-1102, doi: 10.1109/EUMC.2006.281126.
- [7] J. Yao, "Photonic Generation of Microwave and Millimeter-wave Signals," *International Journal of Microwave and Optical Technology*, vol.5 no.1, January 2010. <https://www.ijmot.com/ijmot/uploaded/bf72ylspk88s.pdf>
- [8] E. A. Kittlaus, D. Eliyahu, S. Ganji, et al. "A low-noise photonic heterodyne synthesizer and its application to millimeter-wave radar," *Nat Commun* 12, 4397 (2021). <https://doi.org/10.1038/s41467-021-24637-0>
- [9] A. B. Dar, F. Ahmad, "Optical millimeter-wave generation techniques: An overview," *Optik*, Volume 258, 2022, <https://doi.org/10.1016/j.ijleo.2022.168858>.
- [10] <https://www.vpiphotonics.com/index.php>
- [11] B. Ghosh, S. Mandal, "Fiber Bragg grating-based optical filters for high-resolution sensing: A comprehensive analysis," *Results in Optics*, Volume 12, 2023, <https://doi.org/10.1016/j.rio.2023.100441>.
- [12] F. Zhang and S. Pan, "Microwave photonic signal generation for radar applications," 2016 IEEE International Workshop on Electromagnetics: Applications and Student Innovation Competition (iWEM), Nanjing, China, 2016, pp. 1-3, doi: 10.1109/iWEM.2016.7504991.
- [13] A. Delmade et al., "Optical Heterodyne Analog Radio-Over-Fiber Link for Millimeter-Wave Wireless Systems," in *Journal of*

Lightwave Technology, vol. 39, no. 2, pp. 465-474, 15 Jan.15, 2021, doi: 10.1109/JLT.2020.3032923.

- [14] Wang, L. (2018). Microwave Sensors for Breast Cancer Detection. *Sensors*, 18(2), 655. <https://doi.org/10.3390/s18020655>



Blaise Tshibangu Mbuebue received a B.E. degree in electrical engineering, in the option of computing applied science from the Institut Supérieur de Techniques Appliquées (ISTA/Ndolo), Kinshasa, Congo D.R., in 2010; the M.S. degree in electrical engineering, in the option of instrumentation and digital systems from Universidad de Guanajuato, México, in 2019; and the Ph.D. degree in science with a specialty in electronics at the Instituto Nacional de Astrofísica, Óptica y Electrónica (INAOE), Puebla, México in 2024. His research interests include optical communication system implementations, optical techniques for information transmission through optical fibers, and microwave signal generation. Aspiring member of AMO (Mexican Academy of Optic) in 2019, and IEEE graduate student member of Puebla section since 2021.



Min Won Lee received the MSc degree from Ajou University, Suwon, South Korea in 1998 and the Ph.D. degree from the Université de Franche-Comté, Besançon, France in 2002. His doctoral research was concerned with chaotic dynamics behavior, chaos synchronization, optical telecommunications, and chaos encryption. After his Ph.D., he worked in the Optoelectronic group at Bangor University, United Kingdom from 2002 to 2008. He was involved in the development of chaos communications systems using external-cavity laser diodes. He joined FEMTO-ST Institute, Besançon, France in 2009. His research interests included fiber optical parametric amplifiers, Raman fiber lasers, and Brillouin sensing applications using photonic crystal fibers. He joined as a Lecturer the Laboratoire de Physique des Lasers at the University of Paris 13 in 2011, received a research habilitation (HDR), and became a Senior Lecturer in 2018. His current research interests include semiconductor laser dynamics.



Alejandro García-Juárez was born in Tierra Blanca, Veracruz, México. He received his B.S degree in Electronic Engineering from Universidad Autónoma de Puebla, México in 1998, and his M.S and Ph.D. degrees in Optics with a specialty in optoelectronic systems from the Instituto Nacional de Astrofísica, Óptica y Electrónica, Tonantzintla, México in 1999 and 2005, respectively. He is currently a titular professor-researcher with the Department of Research in Physics of the

Universidad de Sonora, México. His current research interests are primarily in optical fiber communication systems, microwave photonics, wideband antennas, microwave filters, electronics, and optoelectronic systems.



Edgard Yvon Tshishimbi Kanyinda is an engineer in electrical engineering and computer Science option from the Institut Supérieur de Techniques Appliquées (ISTA/Ndolo), experienced computer scientist who built his 11 years of experience within the Central Bank of Congo in the field of computer networks and Telecommunications. Currently teaching at Université Reverend Kim and ISTA/Ndolo, teaching the Computer Networks course. With his experience in the field of computer networks, he has developed his knowledge in the design, implementation, deployment, and security of corporate computer networks on several transmission media (optical fiber, UTP cable, coaxial cable, etc.) thus wireless.



Roberto Rojas-Laguna is a Professor of Calculus, Linear Algebra, Electromagnetic Theory, and Optical Fiber Applications at the Department of Electronic Engineering at División de Ingenierías, Campus Irapuato-Salamanca of Universidad de Guanajuato, Mexico. He is conducting projects on optical fiber sensors, rare-earth-doped fiber lasers, and simulation of non-linear phenomena in optical fibers.



Ignacio Enrique Zaldívar-Huerta received his BS degree (Electronic Engineering) from Universidad Autónoma de Puebla, México in 1992; the MS degree in microelectronics from the Instituto Nacional de Astrofísica, Óptica y Electrónica (INAOE) Puebla, Mexico in 1995; and, the PhD Degree in Sciences for Engineering from the Université de Franche Comté, Besançon, France, in 2001. Since 2002, he has been with the Electronics Department at the INAOE. Currently, he is Titular Researcher. His main research interests are subjects related to optical communications. He has published over 40 articles in international peer-reviewed journals, and 58 papers in international peer-reviewed conferences. He has supervised 30 research graduate students to completion, with 11 at the PhD level and 21 at the Master's level. Since 2002 and 2006, is a member of IEEE and SPIE, respectively. Since 2014 he is a Senior Member of IEEE. He was the Chair of the Communications Society of the IEEE Latin America Region 9, Chapter Puebla, and Chair of the IEEE Puebla Section, México.